

## EPISODIC TRANSIENT GAMMA-RAY EMISSION FROM THE MICROQUASAR CYGNUS X-1

S. SABATINI<sup>1,2</sup>, M. TAVANI<sup>1,2</sup>, E. STRIANI<sup>2</sup>, A. BULGARELLI<sup>3</sup>, V. VITTORINI<sup>1,2</sup>, G. PIANO<sup>1,2,4</sup>, E. DEL MONTE<sup>1</sup>, M. FEROCI<sup>1</sup>, F. DE PASQUALE<sup>5</sup>, M. TRIFOGLIO<sup>3</sup>, F. GIANOTTI<sup>3</sup>, A. ARGAN<sup>1</sup>, G. BARBIELLINI<sup>6</sup>, P. CARAVEO<sup>7</sup>, P. W. CATTANEO<sup>8</sup>, A. W. CHEN<sup>7,9</sup>, F. D’AMMANDO<sup>1,2</sup>, E. COSTA<sup>1</sup>, G. DE PARIS<sup>1</sup>, G. DI COCCO<sup>3</sup>, I. DONNARUMMA<sup>1</sup>, Y. EVANGELISTA<sup>1</sup>, A. FERRARI<sup>9,10</sup>, M. FIORINI<sup>7</sup>, F. FUSCHINO<sup>3</sup>, M. GALLI<sup>11</sup>, A. GIULIANI<sup>7</sup>, M. GIUSTI<sup>1</sup>, C. LABANTI<sup>3</sup>, F. LAZZAROTTO<sup>1</sup>, P. LIPARI<sup>12</sup>, F. LONGO<sup>6</sup>, M. MARISALDI<sup>3</sup>, S. MEREGHETTI<sup>7</sup>, E. MORELLI<sup>3</sup>, E. MORETTI<sup>6</sup>, A. MORSELLI<sup>4</sup>, L. PACCIANI<sup>1</sup>, A. PELLIZZONI<sup>13</sup>, F. PEROTTI<sup>7</sup>, P. PICOZZA<sup>2,4</sup>, M. PILIA<sup>13,14</sup>, G. PUCCELLA<sup>15</sup>, M. PRESTI<sup>14</sup>, M. RAPISARDA<sup>15</sup>, A. RAPPOLDI<sup>8</sup>, A. RUBINI<sup>1</sup>, E. SCALISE<sup>1</sup>, P. SOFFITTA<sup>1</sup>, A. TROIS<sup>1</sup>, E. VALLAZZA<sup>6</sup>, S. VERCELLONE<sup>16</sup>, A. ZAMBRA<sup>7</sup>, D. ZANELLO<sup>12</sup>, C. PITTORI<sup>17</sup>, F. VERRECCHIA<sup>17</sup>, P. SANTOLAMAZZA<sup>17</sup>, P. GIOMMI<sup>17</sup>, S. COLAFRANCESCO<sup>17</sup>, L. A. ANTONELLI<sup>18</sup>, AND L. SALOTTI<sup>19</sup>

<sup>1</sup> INAF/IASF-Roma, I-00133 Roma, Italy

<sup>2</sup> Dip. di Fisica, Univ. Tor Vergata, I-00133 Roma, Italy

<sup>3</sup> INAF/IASF-Bologna, I-40129 Bologna, Italy

<sup>4</sup> INFN Roma Tor Vergata, I-00133 Roma, Italy

<sup>5</sup> ITAB, Via dei Vestini 33, I-66100 Chieti, Italy

<sup>6</sup> Dip. Fisica and INFN Trieste, I-34127 Trieste, Italy

<sup>7</sup> INAF/IASF-Milano, I-20133 Milano, Italy

<sup>8</sup> INFN-Pavia, I-27100 Pavia, Italy

<sup>9</sup> CIFS-Torino, I-10133 Torino, Italy

<sup>10</sup> Dip. Fisica, Università di Torino, Turin, Italy

<sup>11</sup> ENEA-Bologna, I-40129 Bologna, Italy

<sup>12</sup> INFN-Roma La Sapienza, I-00185 Roma, Italy

<sup>13</sup> INAF-Osservatorio Astronomico di Cagliari, località Poggio dei Pini, Strada 54, I-09012 Capoterra, Italy

<sup>14</sup> Dip. di Fisica, Univ. Dell’Insubria, I-22100 Como, Italy

<sup>15</sup> ENEA Frascati, I-00044 Frascati (Roma), Italy

<sup>16</sup> INAF-IASF-Palermo, via U. La Malfa 15, I-90146 Palermo, Italy

<sup>17</sup> ASI Science Data Center, I-00044 Frascati (Roma), Italy

<sup>18</sup> INAF-OAR, via Frascati 33, I-00040, Monte Porzio Catone, Roma, Italy

<sup>19</sup> Agenzia Spaziale Italiana, I-00198 Roma, Italy

Received 2009 November 30; accepted 2010 February 9; published 2010 February 24

### ABSTRACT

Cygnus X-1 (Cyg X-1) is the archetypal black hole binary system in our Galaxy. We report the main results of an extensive search for transient gamma-ray emission from Cygnus X-1 carried out in the energy range 100 MeV–3 GeV by the *AGILE* satellite, during the period 2007 July–2009 October. The total exposure time is about 300 days, during which the source was in the “hard” X-ray spectral state. We divided the observing intervals in 2–4 week periods, and searched for transient and persistent emission. We report an episode of significant transient gamma-ray emission detected on 2009 October 16 in a position compatible with Cyg X-1 optical position. This episode, which occurred during a hard spectral state of Cyg X-1, shows that a 1–2 day time variable emission above 100 MeV can be produced during hard spectral states, having important theoretical implications for current Comptonization models for Cyg X-1 and other microquasars. Except for this one short timescale episode, no significant gamma-ray emission was detected by *AGILE*. By integrating all available data, we obtain a  $2\sigma$  upper limit for the total integrated flux of  $F_{\gamma,\text{U.L.}} = 3 \times 10^{-8}$  ph cm<sup>-2</sup> s<sup>-1</sup> in the energy range 100 MeV–3 GeV. We then clearly establish the existence of a spectral cutoff in the energy range 1–100 MeV that applies to the typical hard state outside the flaring period and that confirms the historically known spectral cutoff above 1 MeV.

*Key words:* gamma rays: general – stars: individual (Cygnus X-1) – X-rays: binaries

### 1. INTRODUCTION

Cyg X-1 is a binary system (discovered by Bowyer et al. 1965) containing an O9.7 Iab supergiant star orbiting (5.6 days of period) around a compact star with a mass function of  $f = 0.23 \pm 0.01 M_{\odot}$  (Gies et al. 2008) and a mass lower limit in the range 6–13  $M_{\odot}$  (Ziółkowski 2005). Cyg X-1 is then the only known high-mass black hole (BH) binary system in our Galaxy (e.g., Tanaka & Lewin 1995), and attracted considerable attention since its initial mass range determinations (Bolton 1972; Webster & Murdin 1972). Being among the brightest X-ray binaries in our Galaxy (for a relatively small distance of 2 kpc and average sub-Eddington X-ray luminosity for a 10 solar-mass compact object), the system has been exten-

sively monitored in the radio, IR, UV, and X-ray energy bands (see Zdziarski & Gierliński 2004 for a review).

The system spends most of its time in the so-called “hard state” characterized by a relatively low flux of soft X-ray photons (1–10 keV), a clear peak of the photon energy spectrum in the hard X-ray band (around 100 keV), and an energy cutoff around 1 MeV (e.g., Gierliński et al. 1997; McConnell et al. 2002; Del Monte et al. 2010). Occasionally, Cyg X-1 changes state shifting its energy power spectrum to a “soft state” characterized by a large flux in soft X-rays, a lower hard X-ray flux, and a tail extending to energies up to 1 MeV and beyond (McConnell et al. 2002). Cyg X-1 is also detected in “intermediate hard states,” which usually show a less intense hard X-ray emission and a shift of the spectral hump toward energies less than 100 keV

(Malzac et al. 2006; Wilms et al. 2006). Variability in Cyg X-1 above 100 keV was observed on several different timescales, from months to milliseconds (e.g., Brocksopp et al. 1999; Ling et al. 1997; Pottschmidt et al. 2003; Zdziarski & Gierliński 2004) and giant outburst episodes have been detected in the 15–300 keV by the Interplanetary Network (Golenetskii et al. 2003) during both spectral states.

Theoretically, accretion processes onto a BH system are extensively studied using Cyg X-1 as a typical example. In particular, disk hydrodynamics and radiative and pair-creation properties of Cyg X-1 have been modeled with particular emphasis on the X-ray range and the highest detectable energies (e.g., Zdziarski 1988; Gierliński et al. 1999; Bednarek & Giovannelli 2007; Zdziarski et al. 2009). Extensive modeling of Cyg X-1 X-ray spectral states has been carried out using Comptonization models (e.g., Titarchuk 1994; Poutanen & Svensson 1996; Coppi 1999) and interpret the historical data available in the literature with a spectral cutoff near 1 MeV. Since the detection of a non-thermal power-law spectral component extending up to  $\sim 1$  MeV energies during the “soft” and “intermediate” states, the issue of determining the variability and highest photon energies from Cyg X-1 has been of crucial theoretical importance. A detection of photon emission well above a few MeV from Cyg X-1 would provide a clear signature of efficient non-thermal acceleration processes occurring in the system that would need to be accounted for in Cyg X-1 models and BH accretion disk modeling.

Before the *AGILE* extensive monitoring of Cyg X-1, only temporally sparse information has been available in the energy range above a few MeV. The gamma-ray instruments on board the *Compton Gamma Ray Observatory (CGRO)* observed the Cygnus region several times (typically with 2–4 week long integrations) during the period 1991–1997. In particular, the EGRET instrument provided an overall upper limit to the flux of  $10 \times 10^{-8} \text{ ph cm}^{-2} \text{ s}^{-1}$  above 100 MeV. EGRET observations occurred always during the “hard” spectral state, and did not cover the “soft” state at all.

The only observation of *CGRO* during a soft state of Cyg X-1 was carried out in 1996 June, following an X-ray alert provided by *RXTE* (Cui et al. 1997). *OSSE* and *COMPTEL* observed Cyg X-1 from 1997 June 14 to 25 and this led for the first time to the detection of a high-energy power law up to about 7 MeV (McConnell et al. 2002). This indication of a power-law component extending to MeV and beyond was also supported in recent years by several *INTEGRAL* observations of Cyg X-1 (Cadolle Bel et al. 2006).

A remarkable, although isolated, TeV flaring event of very high-energy emission above  $\sim 300$  GeV from Cyg X-1 was reported by the *MAGIC* Cherenkov telescope during a set of observations in 2006 (Albert et al. 2007). The reported very high energy (VHE) emission (for a pre-trial significance above  $4\sigma$ ) was detected on 2006 September 24, for about 1 hr (corresponding to an orbital phase of 0.9) during a relatively bright hard X-ray emission phase. Simultaneous *INTEGRAL* data (Malzac et al. 2008) show that the TeV flare from Cyg X-1 was detected  $\sim 1$  day before an intense peak in hard X-rays. However, at the time of the TeV flare, both the soft and hard X-ray emission do not show significant variations or rapid state changes: the spectral state was a “hard” one. This detection of transient and very rapid TeV emission from Cyg X-1 indicates that extreme particle acceleration processes may occur also during a hard spectral state, paving the way to detect non-thermal components also in

states previously believed to be characterized by a cutoff above a few MeV.

In this Letter, we report the *AGILE* search for short (days–weeks) timescale gamma-ray emission from Cyg X-1 in the energy range 100 MeV–3 GeV with a total exposure time of  $\sim 300$  days, during the period 2007 July–2009 mid-October. Our data provide the first long timescale monitoring for this important BH system. A separate paper (Del Monte et al. 2010) addresses the details of the X-ray emission as monitored by *AGILE* and other detectors during our first year of observations.

## 2. *AGILE* 2007–2009 OBSERVATIONS OF CYGNUS X-1 AND DATA ANALYSIS

The *AGILE* mission has been operating since 2007 April (Tavani et al. 2008). The *AGILE* scientific instrument is very compact and is characterized by two co-aligned imaging detectors operating in the energy ranges 30 MeV–30 GeV (*GRID*; Barbiellini et al. 2002; Prest et al. 2003) and 18–60 keV (*Super-AGILE*; Feroci et al. 2007), as well as by an anticoincidence system (Perotti et al. 2006) and a calorimeter (Labanti et al. 2006). *AGILE*’s performance is characterized by large fields of view (2.5 and 1 sr for the gamma-ray and hard X-ray bands, respectively) and optimal angular resolution (PSF =  $3^\circ$  at 100 MeV and PSF =  $1:5$  at 400 MeV). Flux sensitivity for a typical one-week observing period can reach the level of several tens of  $10^{-8} \text{ ph cm}^{-2} \text{ s}^{-1}$  above 100 MeV, and 10–20 mCrab in the 18–60 keV range depending on off-axis angles and pointing directions (see Tavani et al. 2008 for details about the mission and main instrument performance).

The *AGILE* satellite repeatedly pointed at the Cygnus region for a total of  $\sim 315$  days ( $\sim 13$  Ms net exposure) during the period 2007 July–2009 mid-October. The analysis of gamma-ray data presented in this Letter was carried out with the *AGILE-GRID* FT3ab2Build18 calibrated filter with a gamma-ray event selection that takes into account South Atlantic Anomaly event cuts and  $80^\circ$  Earth albedo filtering. Throughout the Letter, statistical significance assessment and source flux determination were established using the standard *AGILE* multi-source likelihood analysis software (A. W. Chen et al. 2010, in preparation). The method provides an assessment of the statistical significance in terms of a Test Statistic (TS) defined as in Mattox et al. (1996) and asymptotically distributed as a  $\chi^2/2$  for 3 degrees of freedom ( $\chi_3^2/2$ ).

### 2.1. Search for Persistent Gamma-ray Emission

Multi-source likelihood analysis was used to search for persistent emission from Cyg X-1 position in the integrated sky map of the Cygnus region above 100 MeV for the period 2007 July–2009 October (Figure 1, upper panel). The region is characterized by *AGILE* gamma-rays data showing two most prominent sources 1AGL J2022+4032 and 1AGL J2021+3652 detected with high confidence ( $38.8\sigma$  and  $24.6\sigma$ , respectively) and a gamma-ray flux  $F_\gamma = (123 \pm 4) \times 10^{-8} \text{ ph cm}^{-2} \text{ s}^{-1}$  and  $F_\gamma = (57 \pm 4) \times 10^{-8} \text{ ph cm}^{-2} \text{ s}^{-1}$ , respectively (Pittori et al. 2009). We also detect Cygnus X-3 ( $3.2\sigma$ ,  $F_\gamma = (10 \pm 3) \times 10^{-8} \text{ ph cm}^{-2} \text{ s}^{-1}$ ; Tavani et al. 2009), and the nearby pulsar source 1AGL J2032+4102 ( $10.8\sigma$ ,  $F_\gamma = (35 \pm 3) \times 10^{-8} \text{ ph cm}^{-2} \text{ s}^{-1}$ ).<sup>20</sup> No statistically significant gamma-ray source is detected at a position consistent with that of Cyg X-1.

<sup>20</sup> *AGILE* flux values are in agreement with the Fermi detections (Abdo et al. 2009a) for common sources.

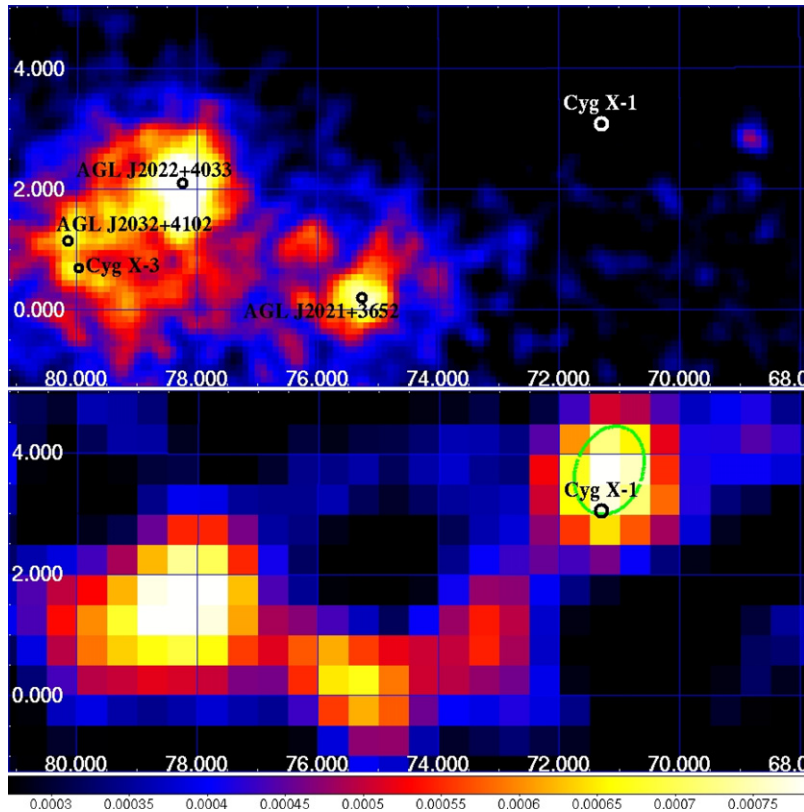


**Figure 1.** *AGILE* gamma-ray intensity maps above 100 MeV of the Cygnus region in Galactic coordinates displayed with a three-bin Gaussian smoothing. Upper panel: *AGILE* 2 years integrated map. Pixel size is  $0.1^\circ$ . We overlaid the nominal position of Cyg X-1 (white circle) and the other sources from *AGILE* catalog. The color bar scale is in units of photons  $\text{cm}^{-2} \text{s}^{-1} \text{pixel}^{-1}$ . Lower panel: *AGILE* 1 day map of the flaring episode of Cyg X-1 (2009-10-15 UTC 23:13:36 to 2009-10-16 UTC 23:02:24). Pixel size is  $0.5^\circ$ . The black circle is the optical position of Cyg X-1 and the green contour is the *AGILE*  $2\sigma$  confidence level.

The  $2\sigma$  upper limit for the gamma-ray flux in the energy range 100 MeV–3 GeV is equal to  $3 \times 10^{-8} \text{ph cm}^{-2} \text{s}^{-1}$ .

Data integrations of 2–4 weeks exposure from single-observation blocks give typical  $2\sigma$  upper limits in the range  $(10\text{--}30) \times 10^{-8} \text{ph cm}^{-2} \text{s}^{-1}$ .

## 2.2. Search for Transient Gamma-ray Emission

Motivated by the X-ray variability of Cyg X-1 and by the particular sequence of flaring gamma-ray emission from Cygnus X-3 (Tavani et al. 2009), we carried out a systematic search for short (day) timescale variability of the Cyg X-1 gamma-ray emission. We used two independent and automatic methods for a blind search of candidate gamma-ray transients in the region surrounding Cyg X-1.

1. *The AGILE-GRID multi-source likelihood method.* The standard analysis pipeline uses a multiple-source likelihood analysis that iteratively optimizes position, flux, and significance of each source by successive repetitions in which the parameters of one source are varied keeping all the others fixed. This method is very efficient for relatively strong sources and takes into account the Galactic diffuse emission and residual background (Bulgarelli et al. 2008). It provides a pre-trial assessment of statistical significance that needs to be corrected when used in repeated systematic searches. For this reason, we also developed an independent method that takes into account multiple comparison corrections (see below).
2. *The false discovery rate method (FDRM).* We developed a detection method based on the false discovery rate technique (FDR; Benjamini & Hochberg 1995; Miller et al.

2001; Hopkins et al. 2002) that is a statistical test taking into account the corrections for multiple testing, as needed for example in repeated systematic searches. The FDRM allows us to control the expected rate of false detections (due to background fluctuations) within a selected sample. The method was adapted to the analysis of *AGILE* gamma-ray data of the Galactic plane (S. Sabatini et al. 2010, in preparation). Given an observed distribution of background counts per pixel (the null hypothesis), the selection is based on choosing pixels characterized by  $p$ -values<sup>21</sup> smaller than a threshold,  $\alpha_{\text{FDR}}$ . The crucial FDRM feature is that a  $p$ -value threshold is *not* fixed a priori (as in traditional statistical methods), but is estimated on the data with the requirement that the rate of false detections, within the selected sample, is the chosen  $\alpha_{\text{FDR}}$  or smaller. A typical value used in the literature (Miller et al. 2001; Hopkins et al. 2002), and that we adopt as a starting value for our search, is  $\alpha_{\text{FDR}} = 0.05$ . The FDRM ensures to control this rate, while accounting for the “post-trial” correction of a single detection significance (Benjamini & Hochberg 1995). We apply the FDRM in two different ways.

*The global-FDRM (G-FDRM).* In this case we carry out a blind search for (persistent or transient) sources in large (*global*) daily count maps of the Galactic plane ( $0.5^\circ$  pixel size). The null hypothesis for these daily maps is the (background-dominated) counts distribution of the Galactic plane ( $|b| \leq 5^\circ$ ). The random fluctuations and the diffuse gamma-ray emission of these daily

<sup>21</sup> Given a statistical distribution, a “ $p$ -value” assigned to a given value of a random variable is defined as the probability, when the null hypothesis is true, of obtaining that value or larger.

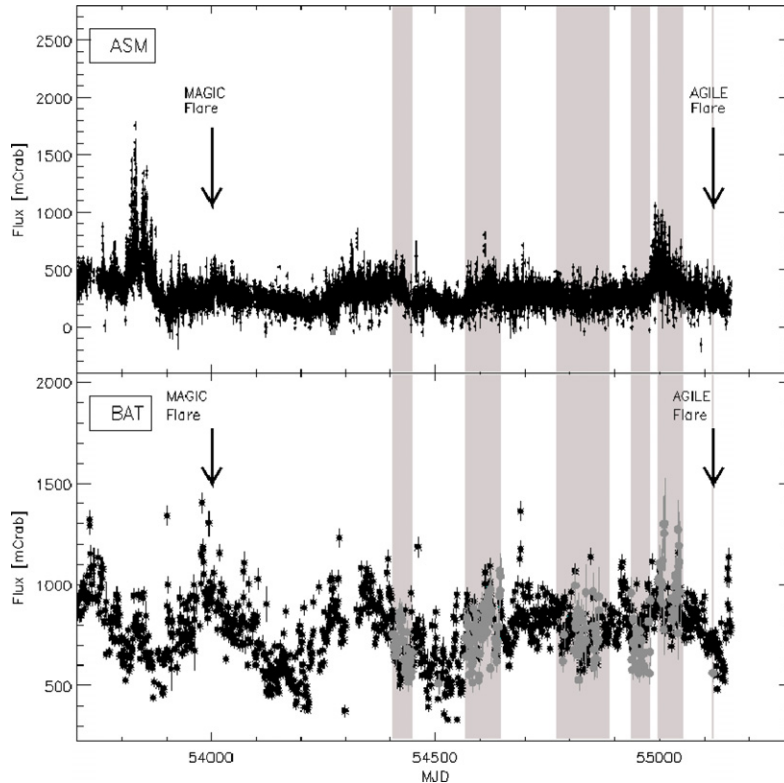


**Figure 2.** Upper panel: *RXTE*/*ASM* daily light curve of Cyg X-1 over the period 2005 November to 2009 October, in the energy range 2–10 keV. The black arrows show the day of *MAGIC* and *AGILE* flaring episodes. Gray regions are *AGILE* pointings of the Cygnus region. Lower panel: *Swift*/*BAT* long-term daily light curve in the energy range 15–50 keV and *Super-AGILE* data (gray dots) when available.

maps are well described by Poissonian distributions in *AGILE*–*GRID* data. Candidate sources in the daily maps are identified as significant deviations from the average distribution that applies to that specific day. In our analysis, we use a threshold of  $\alpha_{\text{FDR}} = 0.05$  that limits the contamination by false positive sources in the sample below 5%.

*The source-FDRM (S-FDRM).* The S-FDRM searches for flaring episodes in the counts’ light curve extracted from the position of a *single* candidate source location. In the (verified) assumption that the average source flux at a given position is typically below the instrument sensitivity, unless it is producing (rare) flares, the null hypothesis in this case is obtained by measuring the distribution of photon counts for the specific sky location observed at intervals of 1 day. We considered the nominal Cyg X-1 position and used an aperture search radius of  $1.5^\circ$ . As in the case for G-FDRM, candidate flaring sources are detected as deviations from the Poissonian average distribution, i.e., fluctuations with  $p$ -value below the chosen threshold.

### 3. THE GAMMA-RAY FLARE OF 2009 OCTOBER 15–16

All of the available *AGILE* data in the archive from 2007 June to 2009 mid-October were searched for variability on timescales of 1 day with both the likelihood and FDR methods. We used only data within  $40^\circ$  from the pointing direction and removed all data affected by non-nominal satellite pointings. In this Letter, we consider only candidates with at least  $5\sigma$  pre-trial significance. Only one gamma-ray flaring episode was definitely detected in our thorough search by both independent methods. The bottom panel of Figure 1 shows the *AGILE* gamma-ray intensity map above 100 MeV for this episode. The emission peaked during the time interval 2009 October 15 (UTC 23:13:36) to 2009 October 16 (UTC 23:02:24). The *AGILE*–

*GRID* multi-source likelihood analysis finds a  $\text{TS} = 28.09$  ( $= 5.3\sigma$  pre-trial,  $4\sigma$  post-trial,<sup>22</sup> according to  $\chi^2/2$  distribution and multiple testing correction) detection at the position  $(l, b) = 71.2, 3.8 \pm 0.7$  (stat)  $\pm 0.1$  (syst) consistent with the position of Cyg X-1, for a gamma-ray flux of  $F_\gamma = (232 \pm 66) \times 10^{-8} \text{ ph cm}^{-2} \text{ s}^{-1}$  in the energy range 100 MeV–3 GeV. The detection is validated by both FDR methods: the G-FDRM analysis finds the source with  $\alpha_{\text{FDR}} = 0.05$  and the S-FDRM analysis with a highly significant  $\alpha_{\text{FDR}} = 0.001$ . G-FDRM detection has a lower significance due to the use of an average background distribution which in this case overestimates the local background. For comparison, during the same time interval the source IAGL J2022+4032 (Pittori et al. 2009), apparently coincident with the supernova remnant Gamma-Cygni, is detected with  $3.1\sigma$  significance with the likelihood analysis (and  $\alpha_{\text{FDR-G}} = 0.05$ ), and a flux of  $F_\gamma = (155 \pm 60) \times 10^{-8} \text{ ph cm}^{-2} \text{ s}^{-1}$ . The *Super-AGILE* (18–60 keV) flux for Cyg X-1 for the day is  $F_{\text{SA}} = (580 \pm 48) \text{ mCrab}$  and the *ASM* flux is  $F_{\text{ASM}} = (268 \pm 20) \text{ mCrab}$  in the 2–12 keV range. The spectral state of the source was determined by means of the color–color diagram obtained from *ASM* data as discussed in Del Monte et al. (2010). Interestingly, the flaring episode (MJD = 55120) occurred during a hard spectral state. The orbital phase of Cyg X-1 was in the range 0.38–0.56. The system was detected to subsequently evolve into one of the relatively rare dips of the hard X-ray light curve.

### 4. DISCUSSION

Figure 2 shows the X-ray historical light curves of Cyg X-1 from 2005 November: the upper panel reports the *RXTE*/*ASM* data, and the lower panel the *Swift*/*BAT* data, superimposed

<sup>22</sup> This corresponds to a  $p$ -value of  $1.7 \times 10^{-6}$  (pre-trial) and  $5.2 \times 10^{-4}$  (post-trial).

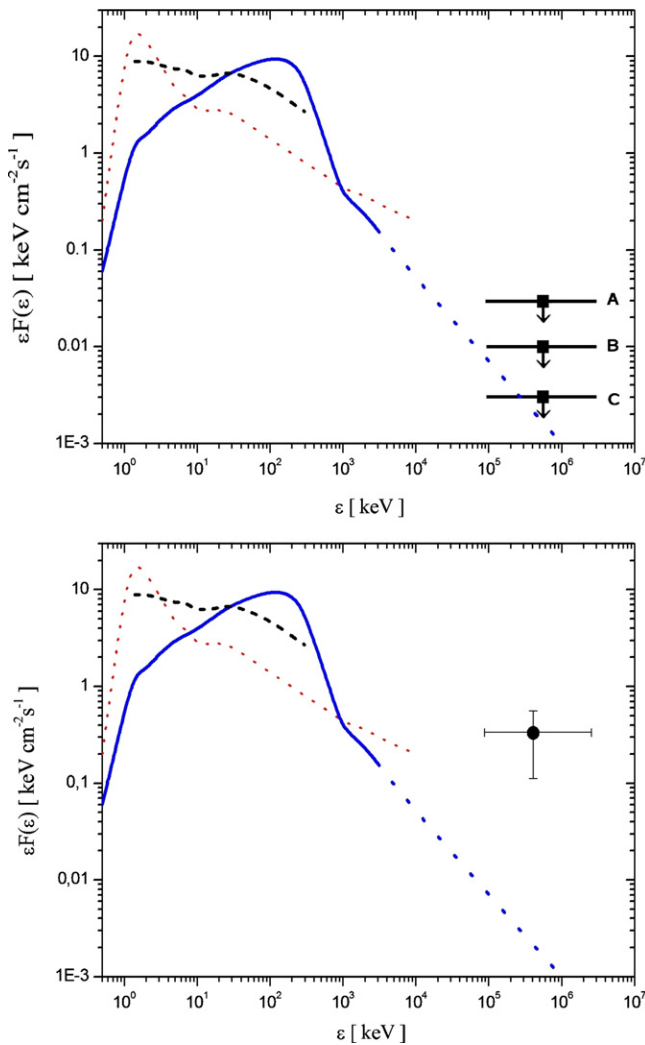


**Figure 3.** Cyg X-1 spectral energy distribution in typical states (“hard” in solid line, “soft” in dotted line, and “intermediate” in dashed line; Gierliński et al. 1999; Zdziarski et al. 2002). The dashed line extrapolated from the hard X-ray state is a purely graphical extension of the trend suggested by the historical data. Upper panel: *AGILE*  $2\sigma$  upper limits above 100 MeV for integration times of two weeks (A), four weeks (B), and  $\sim 315$  days (C). Lower panel: *AGILE* data above 100 MeV for the flaring episode.

with the *Super-AGILE* data from 2007 November (gray dots). Gray zones highlight *AGILE* pointings of the Cygnus region. The ASM data show that after MJD 53900 the system did not undergo clear transitions to one of its soft states anymore. The *Swift*/*BAT* hard X-ray data are available for the last four years and show a pattern with rare dips occurring almost once a year.

The *AGILE* data set extends for  $\sim 300$  days, during which the system was in its typical hard X-ray state (Del Monte et al. 2010). The lack of relatively strong gamma-ray emission on a timescale of weeks together with the deep upper limit obtained by integrating all *AGILE-GRID* data clearly confirms the existence of a spectral cutoff between 1 and 100 MeV in the typical hard state. Figure 3 (upper panel) shows the spectral energy distribution of Cyg X-1 with its typical historical spectral states. In the same figure, typical *AGILE* upper limits are given for two weeks, four weeks, and  $\sim 300$  days integrations. This gamma-ray average spectral behavior of Cyg X-1 in the hard state during week–month timescales is in overall agreement with Comptonization models of BH candidates (e.g., Titarchuk 1994;

Poutanen & Svensson 1996; Coppi 1999) and more specifically of Cyg X-1 (Gierliński et al. 1997; McConnell et al. 2002).

However, our detection of 2009 October 16 is the first reported one-day gamma-ray flare in the energy range 100 MeV–3 GeV from the system during a hard state. This shows that physical processes can occasionally be more complex than predicted by current models. The lower panel of Figure 3 shows the *AGILE-GRID* gamma-ray detection during such flare together with the spectral shapes characterizing the different spectral states for reference. Efficient particle acceleration occurs also in states characterized by the presence of a hot corona that should be in pair-Comptonized equilibrium (e.g., Zdziarski 1988; Zdziarski et al. 2009). The gamma-ray emission can have leptonic or hadronic origin (e.g., Perucho & Bosch-Ramon 2008), depending on the model as well as on the assumptions on the acceleration site (close or far from the inner disk and/or jet). Lack of simultaneous TeV data prevents a more complete spectral analysis of the gamma-ray flaring event. We note that the TeV spectrum reported by *MAGIC* occurred also during a hard state and having a photon spectral index  $\alpha = 3.2 \pm 0.6$  (Albert et al. 2007) is in qualitative agreement with our *AGILE* spectral detection,<sup>23</sup> even though the broadband spectrum may be complex and has several independent components. A theoretical analysis of our results is well beyond the scope of this Letter.

## 5. CONCLUSIONS

*AGILE* extensive monitoring of Cyg X-1 in the energy range 100 MeV–3 GeV during the period 2007 July–2009 October confirmed the existence of a spectral cutoff between 1 and 100 MeV during the typical hard spectral state of the source. However, even in this state, Cyg X-1 is capable of producing episodes of extreme particle acceleration on 1-day timescales. Our first detection of a gamma-ray flare above 100 MeV adds to the even shorter detection in the TeV range by *MAGIC*. These data have great relevance for a more detailed theoretical modeling of pair equilibrium Comptonized coronae and non-thermal particle acceleration that may co-exist for short timescales of order of hours–days.

We note that the gamma-ray flaring activity detected by *AGILE* from Cyg X-1 during its decreasing trend of hard X-ray emission is qualitatively similar (transition to a hard X-ray minimum) to what observed in the case of the other microquasar Cygnus X-3 (Tavani et al. 2009; Abdo et al. 2009b). Whether this behavior is common to microquasars and BH accreting systems is a fascinating question that will be addressed by future observations.

We thank the anonymous referee for the contribution to the improvement of our Letter. The *AGILE* mission is funded by the Italian Space Agency with scientific and programmatic participation by the Italian Institute of Astrophysics and the Italian Institute of Nuclear Physics.

## REFERENCES

- Abdo, A. A., et al. 2009a, *ApJS*, 183, 46A  
 Abdo, A. A., et al. 2009b, *Science*, 326, 1512  
 Albert, J., et al. 2007, *ApJ*, 665, L51  
 Barbiellini, G., et al. 2002, *Nucl. Instrum. Methods Phys. Res. A*, 490, 146  
 Bednarek, W., & Giovannelli, F. 2007, *A&A*, 464, 437

<sup>23</sup> The gamma-ray detection has a flux about a factor of 3 above the model of Zdziarski et al. (2009).

- Belloni, T. M. (ed.) 2009, *Lecture Notes Phys.* 794, *The Jet Paradigm—From Microquasars to Quasars* (Berlin: Springer), 53
- Benjamini, Y., & Hochberg, Y. 1995, *J. R. Stat. Soc. B*, 57, 289
- Bolton, C. T. 1972, *Nature*, 235, 271
- Bowyer, S. C., Byram, E. T., Chubb, T. A., & Friedman, M. 1965, *Science*, 147, 394
- Brocksopp, C., et al. 1999, *MNRAS*, 309, 1063
- Bulgarelli, A., et al. 2008, *ASP Conf. Ser.* 30, *Astronomical Data Analysis Software and Systems* (San Francisco, CA: ASP), 18
- Cadolle Bel, M., et al. 2006, *A&A*, 446, 591
- Coppi, P. S. 1999, in *ASP Conf. Ser.* 161, *High Energy Processes in Accreting Black Holes*, ed. J. Poutanen & R. Svensson (San Francisco, CA: ASP), 375
- Cui, W., et al. 1997, *ApJ*, 474, L57
- Del Monte, E., et al. 2010, *A&A*, submitted
- Feroci, M., et al. 2007, *Nucl. Instrum. Methods Phys. Res. A*, 581, 728
- Gierliński, M., Zdziarski, A. A., Poutanen, J., Coppi, P. S., Ebisawa, K., & Johnson, W. N. 1999, *MNRAS*, 309, 496
- Gierliński, M., et al. 1997, *MNRAS*, 288, 958
- Gies, D. R., et al. 2008, *ApJ*, 678, 1237
- Golenetskii, S., et al. 2003, *ApJ*, 596, 1113
- Hopkins, A. M., et al. 2002, *AJ*, 123, 1086
- Labanti, C., et al. 2006, *Proc. SPIE*, 6266, 62663
- Ling, J. C., et al. 1997, *ApJ*, 484, 375
- Malzac, J., et al. 2006, *A&A*, 448, 1125
- Malzac, J., et al. 2008, *A&A*, 492, 527
- Mattox, J. R., et al. 1996, *ApJ*, 461, 396
- McConnell, M. L., et al. 2002, *ApJ*, 572, 984
- Miller, C. J., et al. 2001, *AJ*, 122, 3492
- Perotti, F., et al. 2006, *Nucl. Instrum. Methods Phys. Res. A*, 556, 228
- Perucho, M., & Bosch-Ramon, V. 2008, *A&A*, 482, 917
- Pittori, C., et al. 2009, *A&A*, 506, 1563
- Pottschmidt, K., et al. 2003, *A&A*, 407, 1039
- Poutanen, J., & Svensson, R. 1996, *ApJ*, 470, 249
- Prest, M., et al. 2003, *Nucl. Instrum. Methods Phys. Res. A*, 501, 280
- Tanaka, Y., & Lewin, W. H. G. 1995, in *X-Ray Binaries*, ed. W. H. G. Lewin, J. van Paradijs, & E. P. J. van den Heuvel (Cambridge: Cambridge Univ. Press), 126
- Tavani, M., et al. 2008, *A&A*, 502, 995
- Tavani, M., et al. 2009, *Nature*, 462, 620
- Titarchuk, L. 1994, *ApJ*, 434, 570
- Webster, B. L., & Murdin, P. 1972, *Nature*, 235, 37
- Wilms, J., Nowak, M. A., Pottschmidt, K., Pooley, G. G., & Fritz, S. 2006, *A&A*, 447, 245
- Zdziarski, A. A. 1988, *ApJ*, 335, 786
- Zdziarski, A. A., & Gierliński, M. 2004, *Prog. Theor. Phys. Suppl.*, 155, 99
- Zdziarski, A. A., Malzac, J., & Bednarek, W. 2009, *MNRAS*, 394, L41
- Zdziarski, A. A., Poutanen, J., Paciesas, W. S., & Wen, L. 2002, *ApJ*, 578, 357
- Ziółkowski, J. 2005, *MNRAS*, 358, 851